

Observation of a breakup-induced α -transfer process for some bound states of ^{16}O populated by the $^{12}\text{C}(^6\text{Li},d)^{16}\text{O}^*$ reaction

S. Adhikari,¹ C. Basu,¹ I. J. Thompson,² P. Sugathan,³ A. Jhinghan,³ K. S. Golda,³ A. Babu,³ D. Singh,³ S. Ray,⁴ and A. K. Mitra¹

¹*Nuclear Physics Division, Saha Institute of Nuclear Physics, Kolkata 700064, India*

²*Lawrence Livermore National Laboratory, L-414, Livermore, California 94551, USA*

³*Inter University Accelerator Centre, New Delhi 110067, India*

⁴*Physics Department, Ramkrishna Mission Vivekananda University, Belur, Howrah, India*

(Received 23 April 2013; revised manuscript received 3 March 2014; published 30 April 2014)

Background: The $^{12}\text{C}(^6\text{Li},d)$ reaction has been used as an indirect method to calculate the astrophysical S factor for the $^{12}\text{C}(\alpha,\gamma)$ reaction at Gamow energy (300 keV).

Purpose: The $^{12}\text{C}(^6\text{Li},d)$ reaction is usually interpreted in terms of direct transfer. In this work we investigate the reaction mechanism and determine the effects of breakup on transfer and therefore on the extracted spectroscopic amplitudes.

Method: The deuteron angular distributions for the $^{12}\text{C}(^6\text{Li},d)^{16}\text{O}^*$ has been measured at 20 MeV, populating discrete states of ^{16}O . continuum discretized coupled channel-coupled reaction channel (CDCC-CRC) calculations have been used to analyze the data.

Results: Results show a new reaction mechanism, where transfer occurs after the breakup of the loosely bound ^6Li in the population of some bound states of ^{16}O . A comparison of the CDCC-CRC calculations with respect to the measured data were used to determine the α spectroscopic amplitudes and factors for the different states of ^{16}O . Using the spectroscopic amplitudes obtained in this work, the $E2$ S factor for the $^{12}\text{C}(\alpha,\gamma)$ reaction has been calculated in the framework of a two-body potential model and compared to measurements.

Conclusions: The present study very clearly shows that the breakup and transfer coupling effects are strong in the $^{12}\text{C}(^6\text{Li},d)$ reaction. The present work extracts, in the framework of a coupled reaction channel theory, the spectroscopic amplitudes of the bound and unbound states of ^{16}O . All previous analysis and new measurements should therefore be reexamined from this viewpoint to extract the astrophysical observables correctly.

DOI: [10.1103/PhysRevC.89.044618](https://doi.org/10.1103/PhysRevC.89.044618)

PACS number(s): 25.70.Hi, 24.10.Eq, 27.20.+n

I. INTRODUCTION

The $^{12}\text{C}(^6\text{Li},d)^{16}\text{O}^*$ reaction has drawn the interest of quite a number of recent works [1–4] in nuclear physics. The reason for this interest lies in the potential of this reaction to determine important astrophysical observables and unravel mysteries of nuclear reaction mechanisms. The availability of sophisticated reaction models in recent times makes a reexamination of the reaction necessary. Most of the earlier works concentrate on the study of reaction mechanism involved either in terms of a direct α -transfer or a compound nucleus model. The reaction mechanism depends upon the kinematics (beam energy, excitation energy, and angle) as well as the structure (spin, parity, and degree of α clustering) of the particular final state. For beam energies of a few MeV per nucleon and forward angles, the direct reaction dominates for most states owing to the loose $\alpha + d$ substructure in ^6Li . It is customary to determine the reaction mechanism from the measurement of deuteron angular distributions populating discrete states of ^{16}O and comparison with reaction models. The direct α -transfer process populating the discrete states of ^{16}O is typically modeled by the finite-range distorted-wave Born approximation (FRDWBA) theory [5]. A discrepancy of the model calculations in comparison to the measured angular distributions at forward angles is accounted in terms of the spectroscopic factor (S_α) [6–8]. The extraction of the α -spectroscopic factor is important as it determines the as-

trophysically relevant quantity, the asymptotic normalization constant (ANC) [4,5]. The astrophysical S factor at the desired low energy can then be calculated in the framework of the R -matrix theory or a potential model. In the potential model, the capture process occurs through an initial scattering state that decays finally to a bound state by emission of γ ray. These states are generated by a suitable potential of the interacting nuclei. The capture reaction at astrophysical energies often occurs through subthreshold states and the magnitude of the tail of the wave function of these states (which determines the ANC) influences the capture cross section and hence the astrophysical S factor. The parameters of the scattering state potential are chosen so as to reproduce the binding energy and ANC of the subthreshold state, using the spectroscopic factor obtained from transfer angular distributions. The ANC or S_α is considered to be important for the 6.92 (2^+)- and 7.12 (1^-)-MeV subthreshold states of ^{16}O [4]. This is because these two states play key roles in the $E2$ and $E1$ capture processes of $^{12}\text{C}(\alpha,\gamma)$ reaction in stars [9].

To extract meaningfully the S_α , and hence the ANC, a clear understanding of the interplay between different reaction mechanisms of the $^{12}\text{C}(^6\text{Li},d)^{16}\text{O}^*$ reaction is needed. As the reaction mechanism is expected to vary strongly with the incident energy, analysis at specific energies is required in terms of the most up-to-date reaction models. An admixture of nondirect reaction mechanism with direct process would mean an incorrect and ambiguous estimate of S_α and ANC

and hence the astrophysical S factor [5]. The nondirect component has been usually considered as a compound nuclear phenomena and is ignored at forward angles where S_α is extracted. However, a loosely bound projectile such as ${}^6\text{Li}$ with a well-defined $\alpha + d$ substructure may undergo breakup (resonant or nonresonant) before the transfer process. We term this possible process as breakup-induced transfer (BIT). Our motivation in this work is therefore to investigate the importance of the BIT mechanism in the ${}^{12}\text{C}({}^6\text{Li},d){}^{16}\text{O}^*$ reaction using an appropriate model.

The deuteron angular distributions are measured for the population of eight discrete states of ${}^{16}\text{O}$ in the ${}^{12}\text{C}({}^6\text{Li},d){}^{16}\text{O}^*$ reaction at 20 MeV incident energy. A continuum discretized coupled channel-coupled reaction channel (CDCC-CRC) calculation is compared to the data to extract the α spectroscopic amplitudes of the different states of ${}^{16}\text{O}$. The spectroscopic amplitudes of the ${}^{16}\text{O}$ ground state and 6.92-MeV state are used in a two-body potential model to calculate the $E2$ S factor of the ${}^{12}\text{C}(\alpha,\gamma)$ reaction at 300 keV.

II. EARLIER WORKS

The deuteron angular distributions for the population of discrete states of ${}^{16}\text{O}$ in the ${}^{12}\text{C}({}^6\text{Li},d){}^{16}\text{O}^*$ reaction at 20 MeV have been measured in only two other earlier works [10,11]. In the first work [10], the data were analyzed only in terms of a simple Legendre polynomial fit. In the latter work [11], transfer reactions initiated on ${}^{12}\text{C}$ by vector-polarized ${}^6\text{Li}$ were studied in terms of the analyzing power only, and cross sections were not presented in this paper. The more recent measurements of the reaction are done at relatively higher energies [2,3,7,12]. All these works except Ref. [3] analyze the deuteron angular distributions in terms of a direct α transfer mechanism in the framework of DWBA. They do not consider the effect of breakup of the loosely bound ${}^6\text{Li}$ on the transfer process. In Ref. [3] the authors examine the effects of the projectile and target excited states on the transfer process in the framework of the CDCC-CRC theory. However, their calculations do not address accurately the instabilities owing to the higher-lying unbound states of ${}^{16}\text{O}$. The angular distribution resulting from their calculations are therefore not in good agreement with the data in general. In this work, we present an improved CDCC-CRC calculation where unbound states are more accurately considered. The different multistep transfer processes considered in the work of Keeley *et al.* [3] viz., transfer via ${}^6\text{Li}$ resonances and excited states of ${}^{12}\text{C}$ and ${}^{16}\text{O}$ do not give a clear picture of how far only breakup influences the transfer mechanism. We therefore investigate only the effect of inclusion or exclusion of ${}^6\text{Li}$ breakup states (resonant and nonresonant) on the observed angular distributions.

III. EXPERIMENTAL DETAILS

The experiment was carried out using the ${}^6\text{Li}$ beam of the 15UD Pelletron facility of IUAC, New Delhi. A $200\ \mu\text{g}/\text{cm}^2$ natural carbon target was used in the experiment. Two ΔE - E solid-state silicon detector telescopes were used for particle identification and measurement of angular distribution at various angles. The two telescopes were stationed on one side

of the beam with a fixed separation of 24° between the two telescopes. The ΔE of both telescopes were $150\ \mu\text{m}$, whereas the thickness of the E detector of the more forward telescope was 5 mm and that of the other was 4 mm. Circular collimators of diameter 5 mm were used for both telescopes and their distance to the target was 130 mm. The solid angle subtended by the detectors was thus about 1.2 msr and the angular uncertainty $\pm 1.1^\circ$. This uncertainty introduces an error in the cross section, where it is changing very rapidly in the detected angular interval. The error is evaluated by calculating the change in cross section in the extent of the angular uncertainty from the neighboring measured cross sections. The beam divergence and angular straggling effects were calculated using the code LISE [13]. In the present work, the error owing to finite solid angle is an important effect in the vicinity of a deep minimum in the cross section when plotted against the emission angle. This error can be estimated by an angle average of the cross section along with an assumption that the minimum occurs at the angle corresponding to the center of the detector. Two monitor detectors of thickness $300\ \mu\text{m}$ were placed on either side of the beam at $\pm 10^\circ$. The monitors were used for absolute normalization of the cross sections. The grazing angle for the ${}^6\text{Li} + {}^{12}\text{C}$ reaction at 20 MeV is 17° in the c.m. Because the monitors were placed within the grazing angle, the elastic scattering cross section required for the normalization was obtained from the Rutherford formula. Therefore, the systematic uncertainty in the experimental data comes from the uncertainty in the determination of the telescope and monitor solid angles only. This is estimated to be about 8%. The reaction products were measured from 27° to 150° in the laboratory with this detector setup inside the 1.5-m general-purpose scattering chamber. A clear separation between the $Z = 1$ isotopes (p, d, t) was achieved in the $2d\ \Delta E$ - E plot.

In Fig. 1 we show the $1d$ spectrum of the deuterons obtained by gating the $2d$ spectrum where discrete states and a continuous bump is observed. The discrete states of ${}^{16}\text{O}$ are populated from two-body reactions that leave the residual nucleus (${}^{16}\text{O}$) in a definite state. The continuous part results

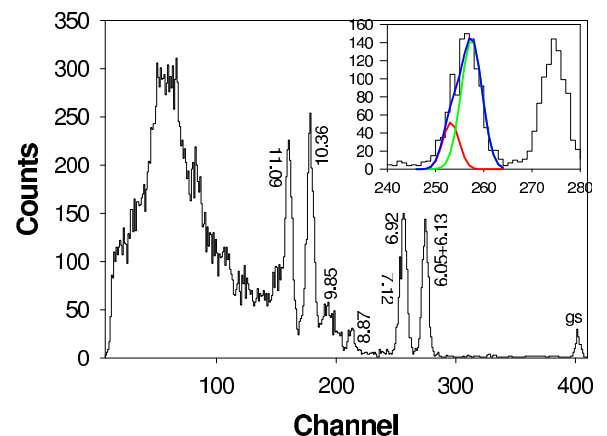


FIG. 1. (Color online) The measured deuteron spectra at 45° showing both the discrete peaks and the continuous bump. A double Gaussian fit to obtain the separate contribution of the 6.92- and 7.12-MeV states is shown in the inset.

from the population of continuum states of ^{16}O or from three-body breakup of the loosely bound projectile ^6Li . The different discrete states of ^{16}O that could be observed are marked in the Fig. 1. The closely spaced 6.92- and 7.12-MeV states that play crucial role in the $E2$ and $E1$ capture process of the $^{12}\text{C}(\alpha, \gamma)$ reaction are seen clearly. The contribution from each state is obtained by performing a double Gaussian fit (considering the background), as shown in the inset of Fig. 1. At angles even where the population of the 7.12-MeV state is much weaker than the 6.92-MeV state, a double Gaussian fit was possible. However, the weaker asymmetry in the peak makes it difficult to determine the 7.12 cross section very accurately. The present measurement also shows a single peak with centroid at 6.13 MeV. It is possible that the two narrowly spaced doublets of 6.05 and 6.13 MeV are not resolved or either of the states is very weakly populated at this energy (20 MeV). In all earlier measurements, a population of 6.13 MeV is stronger than 6.05 MeV and the only other measurement at 20 MeV [10] using magnetic spectrograph showed that the 6.05-MeV peak is very weak in comparison to the 6.13-MeV state. It was also not possible to fit the peak using double Gaussian function with centroids at the desired energies. This indicates that the 6.05-MeV state is probably populated very weakly at this energy (calculations presented later for this doublet are therefore performed considering the 6.13-MeV state only).

IV. RESULTS AND DISCUSSIONS

The measured inclusive deuteron angular distributions converted to the c.m. frame are shown in Figs. 2 and 3 for

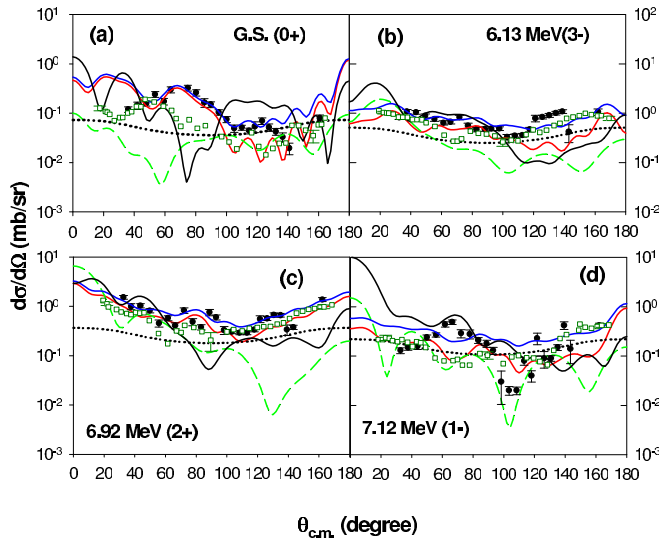


FIG. 2. (Color online) The comparison of the measured angular distributions for the α -bound states of ^{16}O with R -matrix FRDWBA calculations (green dashed lines), Hauser-Feshbach calculations (black dotted lines), and CDCC-CRC (red solid lines) calculations, where all the bound states and unbound resonance states of ^{16}O are considered. The blue solid lines denote the CDCC-CRC calculations summed to the CN component. The black solid lines are the CRC calculations without the breakup channels. The open box symbols are the angular distribution data of Ref. [10].

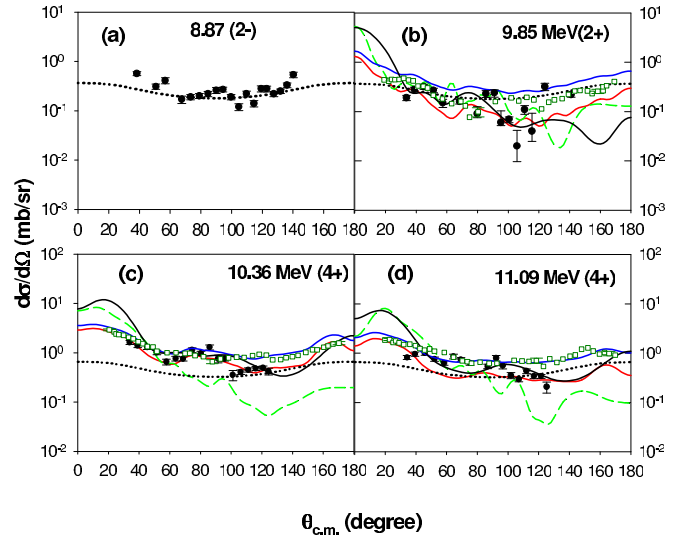


FIG. 3. (Color online) The comparison of the measured angular distributions for the α unbound states of ^{16}O with R -matrix FRDWBA calculations (green dashed lines), Hauser-Feshbach calculations (black dotted lines), and CDCC-CRC (red solid lines) calculations, where all the bound states and unbound resonance states of ^{16}O are considered. The blue solid lines denote the CDCC-CRC calculations summed to the CN component. The 8.87 (2^-)-MeV unnatural parity state is interpreted only in terms of Hauser-Feshbach calculation as this state cannot be populated from direct reactions. The black lines are the CRC calculations without the breakup states. The open box symbols are the same as in Ref. [10].

eight states of ^{16}O . The states of ^{16}O that lie below the $\alpha + ^{12}\text{C}$ threshold (7.16 MeV) are shown in Fig. 2 and those above (unbound states) are shown in Fig. 3. The only other angular distribution data at 20 MeV measured earlier [10] are also shown in Figs. 2 and 3 by open box symbols.

A. Compound nuclear calculations

The compound nuclear (CN) contribution is estimated using the Hauser-Feshbach code CINDY [14] and is shown by dotted lines in Figs. 2 and 3. The required potentials for the calculations are shown in Table I. The 8.87 (2^-)-MeV state is an unnatural parity state and cannot be populated by a direct α -transfer mechanism. A comparison of the Hauser-Feshbach calculations shows that this state is populated through a CN process. As far as the other natural parity states are concerned, the CN process alone cannot explain the entire shape of the angular distributions. It is expected that the forward angle components of the angular distributions are dominated by α -transfer process. This process can proceed either via one-step transfer mechanism from the ground state of ^6Li or after the breakup of the loosely bound projectile.

B. Direct calculations

1. FRDWBA calculations

The direct α -transfer cross sections are calculated in the FRDWBA formalism using the recent version v2.9 of the code FRESKO [5,15]. The required optical potentials in

TABLE I. Potential parameters used in the calculations.

System	V_0 (MeV)	r_0 (fm)	a_0 (fm)	W (MeV)	r_W (fm)	a_W (fm)	V_{so} (MeV)	r_{so} (fm)	a_{so} (fm)	r_c (fm)	Ref.
FRDWBA											
${}^6\text{Li} + {}^{12}\text{C}$	35.0	1.42	1.04	8.46(s)	2.17	0.49	—	—	—	2.5	[20]
$\alpha + {}^{12}\text{C}$	85.9	—	2.8	—	—	—	—	—	—	0.916	[18]
$\alpha + d$	77.2	0.667	0.65	—	—	—	—	—	—	1.3	[19]
$d + {}^{12}\text{C}$	133.6	0.9	0.9	13.78	2.052	0.276	6.0	0.9	0.9	1.303	[17]
CDCC-CRC											
$\alpha + {}^{12}\text{C}$	164.7	1.442	0.52	22.4	1.442	0.52	—	—	—	1.25	[21]
$d + {}^{12}\text{C}$	133.6	0.9	0.9	13.78	2.052	0.276	6.0	0.9	0.9	1.303	[17]
$\alpha + d^a$	77.2	0.667	0.65	—	—	—	1.51	0.667	0.65	1.3	[19]
$\alpha + {}^{12}\text{C}$	85.9	—	2.8	—	—	—	—	—	—	0.916	[18]
CN											
${}^6\text{Li} + {}^{12}\text{C}$	35.0	1.42	1.04	8.46(s)	2.17	0.49	—	—	—	2.5	[20]
$n + {}^{17}\text{F}$	42.13	1.31	0.66	8.619(s)	1.26	0.48	7.0	1.31	0.66	0.0	[22]
$p + {}^{17}\text{O}$	47.067	1.25	0.65	13.5(s)	1.25	0.47	7.5	1.25	0.47	1.25	[23]
$\alpha + {}^{14}\text{N}$	164.7	1.442	0.52	22.4	1.442	0.52	—	—	—	1.25	[21]

^aFor ground-state and nonresonant states of ${}^6\text{Li}$ no spin-orbit term is required; for the 1^+ resonance state V_{so} is 1.51, for the 2^+ state V_{so} is 1.0, and for the 3^+ state V_0 is 80.2 and V_{so} is 1.5.

the FRDWBA calculations are those for the entrance channel (${}^6\text{Li} + {}^{12}\text{C}$), exit channel ($d + {}^{16}\text{O}$), and the core-core ($d + {}^{12}\text{C}$) interactions. The other required real binding potentials are for the ($\alpha + {}^{12}\text{C}$) and ($\alpha + d$) systems. All the potentials used in this work have a Woods-Saxon form factor, except the $\alpha + {}^{12}\text{C}$ binding potential, which has a Gaussian form factor. The parameters of the potentials adopted in the present calculations are from Refs. [10,16] and [17], respectively, for the entrance channel, exit channel, and core-core interactions. The binding potential parameter for ${}^{16}\text{O}$ and ${}^6\text{Li}$ are obtained from Refs. [18] and [19], respectively. All the potentials except the $d + {}^{16}\text{O}$ exit channel optical potential used for all model calculations in this work are shown in Table I. The $d + {}^{16}\text{O}$ optical potential of Ref. [16] has both surface and volume imaginary components ($V_0 = 90.179$ MeV, $r_0 = 1.149$ fm, $a_0 = 0.751$ fm, $W_v = 2.037$ MeV, $W_s = 10.371$ MeV, $r_{W_v} = 1.345$ fm, $r_{W_s} = 1.394$ fm, $a_{W_v} = 0.603$, $a_{W_s} = 0.687$, $V_{so} = 3.557$ MeV, $r_{so} = 0.972$ fm, $a_{so} = 1.011$ fm, $r_c = 1.303$ fm). Another important parameter in the calculation is the number of nodes in the wave functions for ${}^6\text{Li}$ and the different states of ${}^{16}\text{O}$ and they are the same as in earlier works [2,6]. The number of quanta $q = 2n + l$ excited (for each of the states with n nodes and relative angular momentum l) remains almost constant or slightly increases with the excitation energy and is used to choose the n value where an ambiguity exists.

The discrete states of ${}^{16}\text{O}$ above the threshold may result from the $\alpha + {}^{12}\text{C}$ resonances generated by the $\alpha + {}^{12}\text{C}$ binding potential. The resonances can be observed as a rapid increase of the phase shift (δ) when plotted as a function of excitation energy. The $l = 2$ and $l = 4$ phase shifts generated by the $\alpha + {}^{12}\text{C}$ binding potentials are shown in Fig. 4. The depth of the potential is varied to generate the desired resonance in each case. The resonance energy is the energy that corresponds to the maximum slope of the δ vs E curve and the width of the resonance is equal to twice the inverse of the slope at

the resonance energy. The widths of the 9.85-, 10.36-, and 11.09-MeV states are obtained in this method as 0.3, 0.044, and

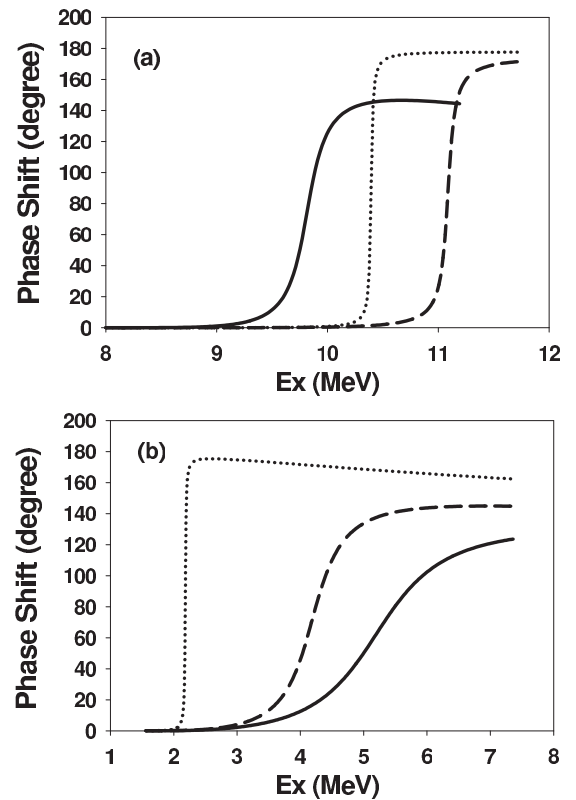


FIG. 4. The phase shift as a function of the excitation energies of (a) ${}^{16}\text{O}$ generated by the Gaussian $\alpha + {}^{12}\text{C}$ binding potential [18] and (b) ${}^6\text{Li}$ generated by the $\alpha + d$ potential [19]. The three resonances of ${}^{16}\text{O}$ and ${}^6\text{Li}$ are shown by solid, dashed, and dotted lines. For details, see text.

0.11 MeV, respectively. In the present FRDWBA calculations we adopt a unit value of the spectroscopic factors for all the ^{16}O states.

The Numerov method generally used in the FRESKO calculations show numerical instabilities when the large Q value unbound states (9.84, 10.36, and 11.09 MeV) are included. In the present work, the R -matrix basis method [5] was used to take care of such instabilities in FRESKO calculations. The number of basis states was determined by studying the convergence of the results. The FRDWBA calculations shown in Figs. 2 and 3 by dashed lines are done by considering 60 R -matrix basis states. The calculations are unable to reproduce the shape of the angular distributions in general. The discrepancy of the direct α -transfer calculations in comparison to the data is usually attributed to the α -spectroscopic factor (S_α). Instead of attributing arbitrary values to S_α in the FRDWBA calculations, we investigate the results from the more complete CDCC-CRC theory.

2. CDCC-CRC calculations

In the present study, owing to the loose binding of the α particle in the projectile, the latter may breakup prior to the α -transfer reaction. This mechanism is termed as BIT in this work. The unique aspect of FRESKO is the CDCC-CRC formalism, a complete theory to consider breakup and transfer reactions in a coupled channel framework. The BIT process is therefore calculated using this feature of the code. In a previous work Keeley *et al.* [3] have used the CDCC-CRC framework to analyze the same $^{12}\text{C}(^6\text{Li}, d)$ angular distributions at higher projectile energies.

In the CDCC-CRC calculations, the ^6Li continuum is divided into three equal bins in the k space with $k_{\text{max}} = 0.78 \text{ fm}^{-1}$. We consider three l values 0, 1, 2 and three resonances of ^6Li at 2.18 MeV (3^+), 4.32 MeV (2^+), and 5.71 MeV (1^+). These resonances are generated by the $\alpha + d$ binding potential and their widths are determined in the same way as for the ^{16}O resonances described before. However, as deuteron has an intrinsic spin of 1, a spin-orbit term was added to the $\alpha + d$ binding potential to split the three $l = 2$ resonances. The widths of the resonant states are found as 0.1 MeV (2.18 MeV), 2.6 MeV (4.32 MeV), and 4.0 MeV (5.71 MeV). The continuum bin size for both ^6Li and ^{16}O should be chosen wide enough so that the entire resonance width calculated from the model falls within the bin. If the actual (experimental) resonance width is narrower than that obtained from the model and is used in the calculations, then the final results will be decreased substantially. However, if the actual width is broader than the calculated width, then the final results will remain unaffected.

In the CDCC-CRC formalism, the entrance channel potential is constructed from the cluster folding of the $\alpha + ^{12}\text{C}$ and $d + ^{12}\text{C}$ potentials. These optical potentials and the other potentials required in the CDCC-CRC calculations are again shown in Table I. However, the imaginary depths of the two potentials required a renormalization to explain the $^6\text{Li} + ^{12}\text{C}$ elastic scattering data [20]. In Fig. 5 we show the comparison of the calculated elastic angular distributions with respect to the data (red line).

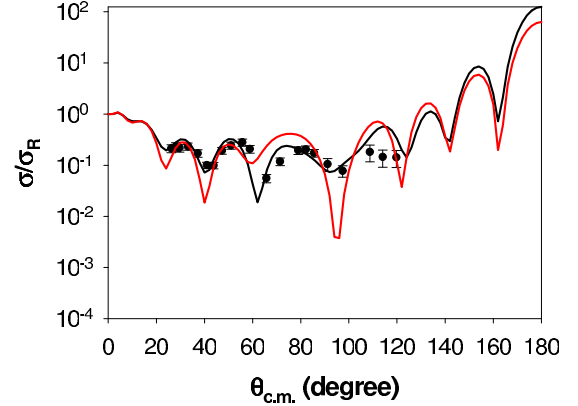


FIG. 5. (Color online) The ratio of the $^6\text{Li} + ^{12}\text{C}$ elastic scattering cross-section data to the Rutherford cross section plotted vs scattering angle. The experimental data are taken from Ref. [24] measured by Ref. [20]. The red line shows the calculation using CDCC-CRC theory with the imaginary part of the $\alpha + ^{12}\text{C}$ and $d + ^{12}\text{C}$ potential parameters as given in Table I renormalized to fit the data. The black line shows the CRC calculation without the breakup channels of ^6Li and requires a different renormalization for the imaginary depth of the $\alpha + ^{12}\text{C}$ and $d + ^{12}\text{C}$ potentials to fit the experimental data.

In the CRC framework, for each intrinsic state $|\alpha\rangle$ FRESKO solves the coupled equations [5]

$$(T - E)\Psi_\alpha + \sum_{\beta} \langle \alpha | V | \beta \rangle \Psi_\beta + \sum_{\beta, x \neq x'} \langle \alpha | \beta \rangle (T - E)\Psi_\beta = 0, \quad (1)$$

where $\Psi_{\alpha, \beta}$ are the relative wave functions of ^6Li with respect to ^{12}C or d with respect to ^{16}O . The intrinsic states $\langle \alpha, \beta |$ are in either of the two mass partitions ($^6\text{Li}, ^{12}\text{C}$) or ($d, ^{16}\text{O}$). In the CDCC-CRC framework we consider all the continuum and resonant states of ^6Li as well as the states of ^{16}O populated in the transfer process. The second term in the equation takes care of all possible couplings between states in the same (inelastic couplings for ^{16}O and breakup couplings for ^6Li) and different (transfer couplings) mass partitions. The third term takes care of the nonorthogonality of states in different partitions. In the transfer coupling the many-body intrinsic states $\langle \alpha |, | \beta \rangle$ can be replaced by a single-particle wave function weighted by the spectroscopic amplitude a . Thus, the spectroscopic amplitudes a (square root of the spectroscopic factors) are the strength of the different states in the solution of the CRC equations that accordingly influence the cross sections. Therefore, unlike in the FRDWBA where the cross sections are proportional to the spectroscopic factor, in the CRC formalism the dependence on the spectroscopic amplitude is not, in general, linear if the coupling effects are strong.

In the present calculations, for example, changing the values of a for a state does not affect the cross section of that state proportionately and weakly affects other states. This result indicates strong transfer and inelastic coupling between the states of ^{16}O and ^6Li as well as between the states of each of these two nuclei. In a strong coupling situation it is very difficult to make a χ^2 search of the a values using the program

TABLE II. Comparison of spectroscopic amplitudes of the ^{16}O states deduced from our calculations with earlier works.

States MeV	Spectroscopic amplitudes		S_α			
	This work	This work	Oulebsir [28]	Bellhout [2]	Bechetti [8]	Keely [3]
0.0	0.32 ± 0.12	$0.10^{+0.09}_{-0.06}$	—	0.34 ± 0.09	$0.38^{+0.02}_{-0.28}$	0.3
6.13	0.22 ± 0.05	$0.05^{+0.03}_{-0.02}$	0.06 ± 0.04	0.29 ± 0.15	$0.09^{+0.03}_{-0.06}$	0.21
6.92	0.32 ± 0.07	$0.10^{+0.05}_{-0.04}$	0.15 ± 0.05	0.37 ± 0.11	$0.17^{+0.06}_{-0.04}$	0.68
7.12	0.22 ± 0.07	$0.05^{+0.04}_{-0.03}$	0.07 ± 0.03	0.11 ± 0.03	$0.08^{+0.04}_{-0.06}$	—
9.85	0.32 ± 0.13	$0.10^{+0.10}_{-0.06}$	$0.10^{+0.08}_{-0.06}$	0.34 ± 0.1	0.002 ± 0.002	—
10.36	0.47 ± 0.16	$0.22^{+0.18}_{-0.12}$	$0.19^{+0.17}_{-0.08}$	0.11 ± 0.06	$0.30^{+0.10}_{-0.06}$	0.617
11.09	0.38 ± 0.11	$0.14^{+0.09}_{-0.07}$	—	—	—	—

SFRESKO. This difficulty is attributable to the impractically long computer times involved in a “fitting” exercise and the nonlinear dependence of the cross section of a state on its spectroscopic amplitude. Instead, we choose different trial values of a for each state and perform CDCC-CRC calculations. The results of the calculation with respect to the experimental angular distribution are used to decide the next set of trial values. The first set of trial values in this process is $a = 1$ for all the states. A guess of the next set is made from the approximate ratio of the experimental to the calculated values of the cross section. Subsequently, one or more a values are changed unless a reasonable agreement to the data is obtained. At each stage, however, the χ^2 values were calculated and for the final results the average value of χ^2/N was found to be less than 20. The final a values that go into the CDCC-CRC calculations for the ^{16}O states are shown in Table II. Also shown are the corresponding α spectroscopic factors (a^2) from this work in comparison to earlier works in the literature.

The overall uncertainty in a (shown in Table II) arises from the error in the angular distribution data, as well from the theoretical errors owing to the uncertainty in the different potential parameters used in the calculations. The theoretical errors in a of a state can be estimated by a variation of the potential parameters and evaluate the corresponding variation in a owing to the variation in the theoretical cross sections. An arbitrary variation of the parameters of the optical potentials is not possible as they are constrained by the elastic scattering data. Similarly, the real potentials for the bound states are constrained by the binding energy and those for the unbound states by their resonance energies.

For the entrance channel in the CDCC model, the $^6\text{Li} + ^{12}\text{C}$ potential is obtained by folding the $\alpha + ^{12}\text{C}$ and $d + ^{12}\text{C}$ optical potentials. It was found from our calculations that when the McFaden-Satchler potential was replaced by another $\alpha + ^{12}\text{C}$ potential [25] the shape of the experimental angular distribution could not be reproduced. However, for a change of the $d + ^{12}\text{C}$ potential, with that prescribed by Daehnick *et al.* [26] the shape of the angular distributions was well reproduced but with a change in the magnitude. The average uncertainties from the entrance channel potential parameters over the entire angular range for the bound states were about 13% and about 30% for the unbound states. Similarly, a

replacement of the $d + ^{16}\text{O}$ exit channel potential by the potential of Daehnick *et al.* results in an uncertainty of about 5%–10%. The uncertainty from the binding potential was about 15%–30% obtained by a variation of the geometry parameter of the binding potential. However, for the unbound states an arbitrary change in the geometry parameter changes the resonance energies and the cross section can reduce dramatically if the resonance width goes out of the chosen bin width. By a variation of the geometry parameters (b) of the Gaussian binding potential [$V = V_0 \exp(-r^2/b^2)$] the agreement of the shape of the calculation with respect to the data for the unbound states changes drastically, putting a constraint on the choice of the potential parameters used in this calculation. In a coupled channel framework owing to the nonlinear relation between the calculated cross section and the spectroscopic amplitude it is not clear how exactly the different sources of errors are related to give the total error in a . However, to make an approximate estimate of the total error we sum in quadrature, the errors from different sources for each i state and this is shown in Table II. As mentioned earlier, a quantitative search for the spectroscopic amplitude is very challenging from the computational point of view and is impractical. Therefore, a qualitative approach, an iterative process relying on educated guesses for appropriate values was carried out. Because the present process to determine a is not based on a least square minimization procedure, it does not provide a defined statistical information. For this reason, definite uncertainties could not be determined from the present method and hence we cannot use statistical measures to compare with the results of other experiments.

The CDCC-CRC calculations performed with 50 R -matrix basis functions and using the spectroscopic amplitudes from Table II are shown in Figs. 2 and 3 (red lines). In comparison to FRDWBA, a much better description of the data was obtained with the CDCC-CRC calculations. A more complete explanation is achieved by adding the CN component to the CDCC-CRC results (blue line).

The improvement with CDCC-CRC calculations over FRDWBA may, however, arise owing to the difference in the entrance channel optical potentials rather than to effects of the breakup channels. In FRDWBA the entrance channel optical potential is a $^6\text{Li} + ^{12}\text{C}$ interaction, whereas in CDCC-CRC the $^6\text{Li} + ^{12}\text{C}$ potential is attributable to a cluster folding of the

$\alpha + {}^{12}\text{C}$ and $d + {}^{12}\text{C}$ potentials. To resolve this problem, we perform the CRC calculations without the breakup channels of ${}^6\text{Li}$ and that have the same incident potential resulting from cluster folding as in CDCC-CRC. The CRC calculations are shown by black lines in Figs. 2 and 3. The spectroscopic amplitudes are chosen so as to obtain the best possible result with respect to the transfer angular distribution data. The elastic scattering calculations from the CRC model are shown by black lines in Fig. 5. The difference of the red and black lines in Figs. 2 and 3 can now be attributed to the projectile breakup effects on the transfer process.

The BIT process is most significant for the population of the ground state. Some contribution of the BIT mechanism is also observed in the population of 6.92- and 6.13-MeV states. However, the population of the other states is primarily by an α -transfer mechanism from the ground state of ${}^6\text{Li}$ (usual transfer process). An extension of the present calculations were carried out at 50 MeV incident energy and compared with the data of Keeley *et al.* [3]. Results show an importance of the BIT mechanism also at this energy most significantly for the ground-state population of ${}^{16}\text{O}$. However, a more elaborate study, to investigate the energy dependence of the BIT process is required for a conclusive understanding.

The results of the present CDCC-CRC calculations (Figs. 2 and 3) in comparison to the earlier data [10] is also satisfactory for most of the states. However, the angular distribution for the population of the ${}^{16}\text{O}$ ground state shows a difference between the present and the earlier measurements [10] beyond 60° in the c.m. frame (see Fig. 2). None of the model calculations (FRDWBA, CDCC-CRC, or CN) could reproduce the shape of Ref. [10], whereas the CDCC-CRC calculations indicate a shape similar to the present measurements. A value of the ground state S_α cannot therefore be determined using the data of Ref. [10]. Similarly, the agreement of the CDCC-CRC calculations for the 7.12-MeV state with either data considering the large angular span seems to be of similar quality and the variation in S_α is difficult to estimate from the variation in the two measurements.

V. ASTROPHYSICAL IMPLICATIONS

A two-body potential model was used to calculate the astrophysical S factor of the ${}^{12}\text{C}(\alpha, \gamma)$ capture reaction at low energies. The calculations were performed with the code FRESKO using the spectroscopic amplitudes obtained from this work for the ${}^{16}\text{O}$ ground state and 6.92-MeV state. The $E2$ S factor corresponding to the ground-state transitions are only calculated because in a two-body model of ${}^{16}\text{O}$, there is no $E1$ component, because the effective charge for the dipole is zero. The $E2$ capture process at astrophysical energies occurs through the tail of the wave function of the 2^+ 6.92-MeV state [27]. The magnitude of the tail of this wave function determines the ANC (C^2) of the state. The ANC is related to the spectroscopic factor (S) of the state and the single particle ANC (b) by the relation ($C^2 = Sb^2$).

In the potential model, we use a $\alpha + {}^{12}\text{C}$ Woods-Saxon (WS) scattering potential in the incident channel. To generate the features of the 6.92-MeV state we varied the potential depth to reproduce its binding energy. The diffuseness parameter of

the WS potential was adjusted to fit an average value of the ANC ($C^2 = 5.11 \pm 1.52 \times 10^{10} \text{fm}^{-1}$) extracted by previous works [2,4,28], while using the spectroscopic factor of the 6.92-MeV state from Table II. The ANC that results from using the single-particle ANC (b) of the Gaussian potential that was used for the α -transfer calculation was not used because the $\alpha + {}^{12}\text{C}$ interaction for transfer at higher energy is not expected to be as peripheral as around 300 keV. Moreover, the Gaussian potential was unable to reproduce the increasing trend of $E2$ S factor at 300 keV, even when the parameters of the potential were adjusted to match the average of the ANC extracted in Refs. [2,4,28]. The potential parameters used to calculate the S factor for the capture via the 6.92-MeV state are $V_0 = 21.8$ MeV, $R = 3.6$ fm, and $a = 1.15$ fm. The $\alpha + {}^{12}\text{C}$ ground-state binding potential is the same as that in our transfer calculations and the number of radial nodes used for the ground-state wave function is 2. The capture calculations were carried out in a coupled channel framework involving an inelastic coupling of the 2^+ (4.43 MeV) state of ${}^{12}\text{C}$ in a rotational model. The deformation parameter $\beta (= -0.02)$ required was rather small for this state. The γ width of the 6.92-MeV state calculated from our model is 20 meV and is of the same order as the experimental value of 96 ± 3 meV [29]. However, the discrepancy between the calculated and the experimental width is a weakness of the present model and may be attributable to the simple two-body ($\alpha + {}^{12}\text{C}$) nature of the state assumed in the calculation.

The calculated $E2$ S factor in comparison to the measured data [30,31] is shown by a red solid line in Fig. 6. At higher energies, however, there is a narrow resonance at 9.84 MeV, which does not influence the energy dependence of the S factor in the astrophysical region. To reproduce the resonance, the potential parameters used were $V_0 = 23.2$ MeV, $R = 3.6$ fm, and $a = 0.7$ fm with $\beta = -0.27$. The coupling effect of the ${}^{12}\text{C}(2^+)$ state is thus important to generate the narrow

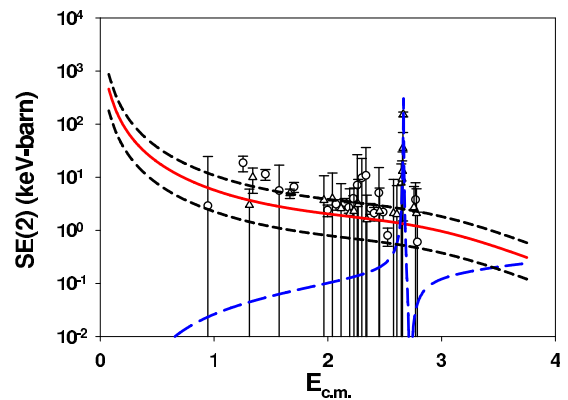


FIG. 6. (Color online) Comparison of potential model calculations of $E2$ S factor with measured data [30,31]. The solid red line and the blue long-dashed line represent the calculations using the potentials which reproduce the features of the 6.92-MeV and the 9.85-MeV 2^+ states, respectively. The spectroscopic amplitudes of the g.s. and 6.92-MeV states that go into this calculation are those evaluated in this work (Table II). The black dashed lines show the value for the S factor owing to the lower and upper limits of ground-state S_α from Table II (for details, see text).

resonance. The calculation of the S factor owing to the $E2$ capture mechanism through this resonance to the ground state is shown by blue dashed line in Fig. 6. A coherent sum involving interference effects [32] could not be carried out in the framework of the simple potential model. Also shown in Fig. 6 (black dashed lines) is the variation in the S factor (when the scattering state reproduces the features of the 6.92-MeV state) owing to the upper and lower limits of ground-state S_α from Table II. The value of $SE2(300)$ from the present calculations comes to about 48 ± 29 keV b. The error in the S factor is estimated by summing in quadrature the error of the alpha spectroscopic factor of the ground state, evaluated in the present work (shown in Table II) and uncertainty in C^2 of the 6.92-MeV state. A χ^2 fitting of higher-quality angular distribution data with those obtained via the present theoretical approach would reduce the errors in S_α and hence the error in the evaluated astrophysical $E2$ S factor, but would be too computationally challenging. The table includes also the value of S factors evaluated in earlier works [4,28,33]. We see that the present method also provides a reasonable estimate of the $SE2$ factor at 300 keV. The effect of breakup is found to be substantial in the spectroscopic factor for the ground state, which is involved in the calculation of astrophysical S factor in the present model.

VI. SUMMARY AND CONCLUSIONS

The population of eight discrete states of ^{16}O are analyzed in terms of the CRC theory including and excluding the breakup of ^6Li . Both the calculations were done using the R -matrix basis expansion method as Numerov solutions are unstable when α unbound states were included. The present study very clearly

shows that the breakup and transfer coupling effects are strong in the $^{12}\text{C}(^6\text{Li},d)$ reaction. A breakup-induced α -transfer (BIT) process is thus significant for some of the bound states of ^{16}O . This also poses a limitation on the application of FRDWBA theory straightaway in the extraction of α spectroscopic factor or ANC of the ^{16}O states, as has been done by earlier works. The present work extracts, in the framework of a coupled-reaction channel theory, the spectroscopic amplitudes of the bound and unbound states of ^{16}O with a minimum variation of parameters. The extracted spectroscopic amplitudes when used in a potential model provide a reasonable estimate of the astrophysical S factor at 300 keV. All previous analysis based on FRDWBA theory [2,6–8] and new measurements should therefore be reexamined from this viewpoint to extract the astrophysical observables correctly. It should be noted, however, that conclusions reached in these previous works depending on ratios of spectroscopic factors would most likely be little changed.

ACKNOWLEDGMENTS

We acknowledge with thanks the wholehearted support from the Pelletron staff of the Inter University Accelerator Centre, New Delhi. We would also like to thank Professor P. Basu, SINP, Kolkata, for providing some of the detectors and the target laboratory, Variable Energy Cyclotron Centre, Kolkata, for providing the targets. S.A. would like to acknowledge financial support from the Department of Science & Technology, India, under Grant No. SR/WOS-A/PS-50/2011. This work was also performed under the auspices of the U.S. Department of Energy by Lawrence Livermore National Laboratory under Contract No. DE-AC52-07NA27344.

-
- [1] S. Adhikari and C. Basu, *Phys. Lett. B* **704**, 308 (2011).
 - [2] A. Belhout *et al.*, *Nucl. Phys. A* **793**, 178 (2007).
 - [3] N. Keeley *et al.*, *Phys. Rev. C* **67**, 044604 (2003), and references therein
 - [4] C. R. Brune, W. H. Geist, R. W. Kavanagh, and K. D. Veal, *Phys. Rev. Lett.* **83**, 4025 (1999).
 - [5] I. J. Thompson and F. M. Nunes, *Nuclear Reactions for Astrophysics* (Cambridge University Press, Cambridge, UK, 2009).
 - [6] F. D. Bechetti *et al.*, *Nucl. Phys. A* **305**, 313 (1978).
 - [7] F. D. Bechetti *et al.*, *Nucl. Phys. A* **344**, 336 (1980).
 - [8] F. D. Bechetti *et al.*, *Nucl. Phys. A* **305**, 293 (1978).
 - [9] G. Imbriani *et al.*, *Astrophys. J.* **558**, 903 (2001).
 - [10] K. Meier-Ewert, K. Bethge, and K. O. Pfeiffer, *Nucl. Phys. A* **110**, 142 (1968).
 - [11] M. Makowska-Rzeszutko *et al.*, *Phys. Lett. B* **74**, 187 (1978).
 - [12] T. L. Drummer, E. E. Bartosz, P. D. Cathers, M. Fauerbach, K. W. Kemper, E. G. Myers, and K. Rusek, *Phys. Rev. C* **59**, 2574 (1999).
 - [13] O. Tarasov *et al.*, *Nucl. Phys. A* **701**, 661c (2002).
 - [14] E. Sheldon and V. C. Rogers, *Comput. Phys. Commun.* **6**, 99 (1973).
 - [15] I. J. Thompson, *Comput. Phys. Rep.* **7**, 167 (1988).
 - [16] H. An and C. Cai, *Phys. Rev. C* **73**, 054605 (2006).
 - [17] H. Wilsch and G. Clausnitzer, *Nucl. Phys. A* **160**, 609 (1971).
 - [18] C. A. Bertulani, *Phys. Rev. C* **49**, 2688 (1994).
 - [19] K. I. Kubo and M. Hirata, *Nucl. Phys. A* **187**, 186 (1972).
 - [20] K. Bethge, K. Meier-Ewert, and K. O. Pfeiffer, *Z. Phys.* **208**, 486 (1968).
 - [21] L. Mcfadden and G. R. Satchler, *Nucl. Phys.* **84**, 177 (1966).
 - [22] D. Wilmore and P. E. Hodgson, *Nucl. Phys. A* **55**, 673 (1964).
 - [23] F. G. Perey, *Phys. Rev.* **131**, 745 (1963).
 - [24] J. W. Watson, *Nucl. Phys. A* **198**, 129 (1972).
 - [25] V. Avrigeanu, P. E. Hodgson, and M. Avrigeanu, *Phys. Rev. C* **49**, 2136 (1994).
 - [26] W. W. Daehnick, J. D. Childs, and Z. Vrcelj, *Phys. Rev. C* **21**, 2253 (1980).
 - [27] C. E. Rolfs and W. S. Rodney, *Cauldrons in the Cosmos – Nuclear Astrophysics* (University of Chicago Press, Chicago and London, 1988).
 - [28] N. Oulebsir *et al.*, *Phys. Rev. C* **85**, 035804 (2012).
 - [29] D. R. Tilley, H. R. Weller, and C. M. Cheves, *Nucl. Phys. A* **564**, 1 (1993).
 - [30] R. Kunz, M. Jaeger, A. Mayer, J. W. Hammer, G. Staudt, S. Harissopulos, and T. Paradellis, *Phys. Rev. Lett.* **86**, 3244 (2001).
 - [31] M. Assuncao *et al.*, *Phys. Rev. C* **73**, 055801 (2006).
 - [32] D. B. Sayre, C. R. Brune, D. E. Carter, D. K. Jacobs, T. N. Massey, and J. E. O'Donnell, *Phys. Rev. Lett.* **109**, 142501 (2012).
 - [33] P. Tischhauser *et al.*, *Phys. Rev. C* **79**, 055803 (2009).